

UCSF

UC San Francisco Electronic Theses and Dissertations

Title

The role of osteoclasts in the development of Class III skeletal malocclusions

Permalink

<https://escholarship.org/uc/item/55k6t2k0>

Author

Cozin, Matthew Joseph

Publication Date

2016

Peer reviewed|Thesis/dissertation

The role of osteoclasts in the development of Class III skeletal malocclusions.

by

Matthew Joseph Cozin DDS

THESIS

Submitted in partial satisfaction of the requirements for the degree of

MASTER OF SCIENCE

in

Oral Craniofacial Sciences

in the

GRADUATE DIVISION of the UNIVERSITY OF CALIFORNIA, SAN FRANCISCO

Dedication and Acknowledgements

This thesis is dedicated to both my family and my research mentor Dr. Andrew Jheon.

My father, Mark Cozin, mother, Sybil Cozin, and brothers Ben and Andrew, have always been there to support me during my long journey through school and residency. Ensuring I was in good health, was happy, lending an ear when I needed to vent, and giving advice when I needed it. My girlfriend Dr. Yu-Hsing Kao has also been there to help me get through the difficult times during residency and ensuring I had food when there was lots of work to do.

My thesis would not have been possible without my research mentor Dr. Andrew Jheon. He has put so much time and energy into my project. During the last two weeks, he would read over my drafts and get revisions back to me within hours. Not only was he extremely supportive with my research project, but he has been a great coresident and friend.

Abstract

Craniofacial skeletal disharmonies present some of the most difficult challenges to orthodontists. Correcting class II (e.g., mandibular retrognathism) and class III (e.g., mandibular prognathism) skeletal discrepancies frequently requires extractions or orthognathic surgery. It is yet unclear how skeletal malocclusions arise but there is evidence for a genetic basis. However, the role of environment and local factors in determination of mandibular length is unknown, but the balance between bone formation and resorption likely influences mandibular length. Experiments performed in avian models [1] where the presence and/or activity of osteoclasts during craniofacial development was inhibited showed effects on beak lengths. For example, inhibition of osteoclasts or bone resorbing cells using the bisphosphonate alendronate during early development (e.g., before mineralization of craniofacial bones) led to an increase in lower beak length (e.g., sagittal length). Conversely, activation of osteoclasts led to a decrease in lower beak length. From these results, we hypothesize that alteration of osteoclasts during development leads to effects on mandibular length in mammals. To test this hypothesis, we employed 2 distinct methods in mice: 1) we inhibited osteoclasts with alendronate *in utero* at E12.5; and 2) we eliminated osteoclasts by generating $Ctsk^{Cre};DTA^{fl/+}$ mice. The second method would reduce osteoclasts by the expression of diphtheria toxin (DTA) wherever *Ctsk* or cathepsin K, an osteoclast marker, is expressed. Specimens were scanned using micro-computed tomography and cephalometric analyses performed. Alendronate treatment *in utero* resulted in slightly increased sagittal length of the mandible. $Ctsk^{Cre};DTA^{fl/+}$ mice had slightly smaller mandibles and cranial base bones relative to their overall size due to a surprising increase in osteoclasts compared to controls. These data will lay the foundation for future experiments to further understand the role of osteoclasts in determination of mammalian mandibular lengths.

Table of Contents	Page
BACKGROUND.....	1
MATERIALS AND METHODS.....	7
RESULTS.....	11
DISCUSSION.....	15
CONCLUSIONS.....	19
REFERENCES.....	20
LIST OF FIGURES.....	23

List of Figures	Page
Figure 1. Bone resorption controls lower beak length.	23
Figure 2. Mouse intraperitoneal injections.	24
Figure 3. <i>In situ</i> hybridization of E14.5 mouse embryos.	25
Figure 4. Generation of <i>Ctsk</i> ^{Cre} ;DTA ^{fl/+} mice.	26
Figure 5. H&E and tartrate-resistant acid phosphatase (TRAP) activity staining of mouse mandibular bone formation at E18.5.	27
Figure 6. Detailed microCT reconstructions of a control male mouse skull.	28
Figure 7. Morphometric comparison of control and <i>Ctsk</i> ^{Cre} ;DTA ^{fl/+} male with anatomical abnormalities.	29
Figure 8. microCTs of mouse skull samples.	30
Figure 9. Amira Landmarks.	31
Figure 10. Sagittal Mn jaw measurement from Co to Pg in control and alendronate-treated mice.	32
Figure 11. Vertical Mn jaw measurement from Co to Go in control and alendronate-treated mice.	33
Figure 12. Sagittal Mn jaw measurement from Go to Pg in control and alendronate-treated mice.	34
Figure 13. Cranial base measurement from Ba to Occ in control and alendronate-treated mice.	35
Figure 14. Cranial base measurement from Occ to S in control and alendronate-treated mice.	36
Figure 15. Sagittal Mn jaw measurement from Co to Pg in control and <i>Ctsk</i> ^{Cre} ;DTA ^{fl/+} mice.	37
Figure 16. Vertical Mn jaw measurement from Co to Go in control and <i>Ctsk</i> ^{Cre} ;DTA ^{fl/+} mice.	38
Figure 17. Sagittal Mn jaw measurement from Go to Pg in control and <i>Ctsk</i> ^{Cre} ;DTA ^{fl/+} mice.	39
Figure 18. Cranial base measurement from Ba to Occ in control and <i>Ctsk</i> ^{Cre} ;DTA ^{fl/+} mice.	40
Figure 19. Cranial base measurement from Occ to S in control and <i>Ctsk</i> ^{Cre} ;DTA ^{fl/+} mice.	41

Background

The development of class II and class III skeletal disharmonies is a significant problem in orthodontics. Class II and III skeletal malocclusions prolong treatment lengths for patients, necessitate more chair time in the office, often involve adjunctive mechanics, and increase the need for extractions and/or orthognathic surgery [2, 3]. It is estimated that as high as 19.2% of patients who present to orthodontists have skeletal disharmonies that need to be treated with orthognathic surgery to achieve an ideal result [4]. Due to monetary reasons, insurance coverage, invasiveness, and possible complications of surgeries, a significantly lower percentage of patients have surgery. In 1907, Angle published his famous book on malocclusion where he studied the relationship of maxillary and mandibular teeth in 1,000 Caucasian subjects [5]. Overall, class II and class III malocclusions made up 23% and 3.4% respectively of this group. Since then, numerous studies have been published on more diverse patient populations, which show that on the whole Angle's study was fairly accurate in regards to class II patients but underestimated the prevalence of class III patients. This was due to the study being limited to the Caucasian population. An aggregate from multiple studies has determined that 27.9% of the US populations have skeletal malocclusions with different severity levels [6].

Orthodontics has progressed through a series of conceptual stages over the past 100 years. During this century of development there has always been the ongoing debate about the relative importance of nature or heredity versus effects from the local environment [7]. In the 19th century, malocclusion was thought to be the result of "pressure habits" as well as dietary deficiencies, endocrine malfunction, and even mental degeneracy [7]. Few dentists considered malocclusions to be hereditary. It was not until the 1960's that genetics and malocclusion were discussed in the American Journal of Orthodontics and the Angle Orthodontist [7].

During the late 1990s and early 2000s, numerous genes were identified as being related to controlling the morphogenesis and growth of craniofacial tissues [7]. A recent report in the Journal of Dental Research analyzed an array of gene candidates from 269 untreated adults to determine if single nucleotide polymorphisms (SNP) were associated with craniofacial features [8]. Their findings suggest that minor alleles of *FGFR2* (fibroblast growth factor receptor 2) were associated with skeletal class II malocclusions whereas individuals with *EDNI* (endothelin-1) SNPs had decreased risk of developing a class II malocclusion. Skeletal class III risk increased with SNPs of *FGFR2* and *COL1A1* (collagen type 1A). *TBX5* (T-Box 5) SNPs were associated with a decreased risk of class III malocclusion [8].

Perillo *et al.* [9] used whole-exome sequencing to analyze the genetic composition of an Italian family of which 30% of the family members presented with class III malocclusions. Five genes with missense variants were found and the Gly1121Ser variant in *ARHGAP21* (Rho GTPase Activating Protein 21) gene was found to be shared by all prognathic individuals studied in this family [9]. Ikuno *et al.* [10] recruited 240 people with mandibular prognathism and 360 control individuals from Japan to identify susceptibility genes involved in mandibular prognathism. Polymerase chain reaction (PCR) was used to amplify the genome from each study subject and the researchers performed a genome-wide association study (GWAS) using 23,465 microsatellite markers to detect mandibular prognathism susceptibility regions. The study identified two chromosome areas; 1q32.2 and 1p22.3, which are likely to be susceptibility regions of mandibular prognathism, *PLXNA2* and *SSX2IP* are the genes closely associated with these two regions. Neither of these genes had previously been linked to craniofacial growth [10].

Matrilin-1(MATN1), a cartilage matrix protein, has been shown to be associated with class III malocclusions when an individual has a specific SNP in *MATN1*. A Korean study

showed that individuals with this *MATN1* SNP had a significantly higher odds ratio (9.28) of developing a skeletal class III malocclusion. Interestingly, another SNP of the same gene had protective effect on developing a class III (OR = 0.16) [11].

Bone development and homeostasis are controlled by a well understood but complex signaling system. Two major cells in the system are the bone-resorbing osteoclasts and bone-forming osteoblasts, which deposit extracellular matrix that eventually mineralizes to form bone. Bone turnover, where old bone is replaced with new bone occurs continuously throughout life, requires precise control and balance. When precise regulation of bone turnover malfunctions, there are numerous downstream effects. For example, when bone formation exceeds resorption, this leads to osteopetrosis, a rare condition in which bone is abnormally dense and prone to fractures. Conversely, one of the most common diseases in elderly men and women is osteoporosis, a metabolic bone disease where the amount of osteoclast function exceeds that of the osteoblasts leading over time to decreased bone density. The most commonly prescribed drugs for osteoporosis are bisphosphonates.

Bisphosphonates are a class of drugs that are synthetic analogs of pyrophosphate, and these compounds have a high affinity for hydroxyapatite observed primarily in bone [12]. These drugs are indicated for the prevention and treatment of hypercalcemia of malignancy, Paget disease of bone, multiple myeloma, and bone metastases associated with breast, prostate, lung, and other soft tissue tumors, as well as postmenopausal and steroid-induced osteoporosis. Bisphosphonates are categorized into 2 major classes: nitrogen-containing and non-nitrogen-containing [12]. Nitrogen-containing bisphosphonates act by inhibiting the farnesyl pyrophosphatase enzyme of the mevalonate pathway, which is involved in the synthesis of

cholesterol, and the prenylation of small G proteins known to be critical in several cellular functions, such as proliferation, cellular migration, and ultimately, wound healing [12].

Cathepsin K (*Ctsk*) is an important protease responsible for degrading type I collagen, osteopontin, and other bone matrix proteins [13]. Specifically, *Ctsk* is highly expressed in osteoclasts and plays a critical role during the osteoclast mediated bone resorption process. This process is very important for many dental developmental mechanisms. For example, the region between the alveolar bone and the cementum of the tooth can be defined as the tooth-bone interface [13]. The specific role of CTSK in osteoclasts during bone resorption occurs through the following mechanism. In mature osteoclasts, CTSK is synthesized as an inactive proenzyme and cleaved by autoproteolysis to produce the active form of the protein. This active form is then secreted into the extracellular lysosome, where it degrades bone matrix proteins, particularly type I collagen, which constitutes 95% of the organic bone matrix. CTSK deficiency does not affect the function of osteoclast-mediated extracellular acidification. *Ctsk* mutations were found to impair the ability of osteoclasts to degrade collagen rather than demineralize the extracellular matrix [14, 15].

Acid phosphatase 5, tartrate resistant (*Acp5*) is a member of a class of purple iron-containing proteins that are distributed widely in nature [16]. *Acp5* is also known as tartrate-resistant acid phosphatase (TRAP) and is released by the ruffled membrane interface at the bone resorptive surface of osteoclasts. In addition, TRAP has been shown to catalyze peroxidation reactions resulting in reactive oxygen species that are important molecules in microbial defence [17, 18]. TRAP activity staining has become common protocol for identifying mature osteoclasts in tissue sections.

Investigation into the role of bone-resorbing osteoclasts on regulating lower beak (or jaw) length in an avian model has been previously studied [1]. This study arose from the observation that there was greater amount of TRAP activity in developing quail beaks compared to duck beaks. TRAP activity is an indicator of osteoclasts and their activity. Because quails possess much shorter beaks than ducks, the authors wanted to test whether osteoclasts may play a role in the determination of avian beak lengths. To test this hypothesis, a single dose of bisphosphonate, specifically alendronate, was injected into the blood vessels of quail embryos *in ovo* before the presence of mineralized craniofacial bone at Hamburger and Hamilton (HH) stage 33 to decrease osteoclast number and/or activity. In addition, osteoprotegerin (OPG) protein or an MMP-13 (metalloproteinase -13) inhibitor, which leads to decreased osteoclasts and activity, was separately injected into quails at HH33. All three treatments (i.e., alendronate, OPG, MMP-13 inhibitor) led to an increase in lower beak length (Figure 1). Conversely, injection of recombinant RANKL (receptor activator of nuclear factor kappa-B ligand), which leads to an increase in osteoclasts, resulted in shorter lower beaks. These results demonstrate the importance of bone resorption, specifically osteoclasts and their activity, in the determination of species-specific beak length. Thus, osteoclast inhibitors resulted in a prognathic lower beak. From these results, it was concluded that inhibition or activation of bone resorption could significantly lengthen or shorten the beak, respectively [1].

The purpose of my study was to determine whether inhibition of osteoclast activity during mammalian development leads to changes in jaw relationships like that observed in avians. Specifically, we hypothesize that inhibition of osteoclast activity *in utero* results in mandibular prognathism and class III skeletal malocclusions. To test our hypothesis, we inhibited osteoclast activity in two ways during mouse development. First, we administered

bisphosphonates *in utero* to inhibit osteoclasts during mouse embryogenesis. Briefly, a single bolus of alendronate was injected intraperitoneally in pregnant mice at embryonic day 12.5 (E12.5) and the craniofacial morphology of the offspring analyzed. Second, we utilized transgenic mouse lines to eliminate osteoclasts. *Ctsk*^{Cre} mice [19] were crossed with ROSA26^{DTA176} [20] to generate mice expressing DTA176 under control of the *Ctsk* promoter (*Ctsk*^{Cre};DTA^{fl/+}). In these mice, expression of the DTA176, which encodes an attenuated diphtheria toxin, eliminates the cells that normally express *Ctsk*, including osteoclasts. Therefore, our two approaches to decrease osteoclasts and/or their activity include an external treatment (i.e., injection), as well as a genetic method (i.e., *Ctsk*^{Cre};DTA^{fl/+} mice). By studying alendronate-treated or transgenic mice, we hypothesize that the inhibition of osteoclasts and bone resorption during mammalian development leads to the development of Class III skeletal malocclusion.

Materials and Methods

Animals

All experimental procedures involving mice were approved by the Institutional Animal Care and Use Committee (IACUC) at UCSF and the mice were handled in accordance with the principles and procedure of the Guide for the Care and Use of Laboratory Animals under the approved protocol AN084146-02F. Mice were maintained in a temperature-controlled facility with access to food and water *ad libitum*. A male and female FVB inbred mouse (Charles River) at 6 weeks of age were mated to generate time-pregnant mice. The presence of a vaginal plug was designated as embryonic day (E) 0.5. Bisphosphonate injections were performed at E12.5 (Figure 2). For analyses of transgenic mice, mice carrying the *Ctsk*^{Cre} [19] and ROSA26^{DTA176} [20] alleles were mated to generate *Ctsk*^{Cre};DTA^{fl/+} offspring. Cre- or DTA197-null littermates were used as controls (Figure 4). Both male and female mice were analyzed at 3 months of age.

Bisphosphonate injections

Alendronate was obtained from Sigma Aldrich (Carlsbad, CA) and reconstituted in 100% ethanol. Pregnant FVB mice at E12.5 were injected intraperitoneally with 1mg/kg of alendronate (experimental group) or 0.9% saline (control group)(Figure 2).

Histology, TRAP staining, and *in situ* hybridization

Mice at 6 weeks of age slated for analyses were euthanized following standard IACUC protocols. Heads were collected, the skin removed, fixed overnight in 4% paraformaldehyde at 4°C for 24-48h, demineralized in 0.5M EDTA for 14 days, dehydrated, embedded in paraffin wax, and serially sectioned at 7µm. Histological sections were stained with haematoxylin and eosin (H&E). For TRAP staining, we used the Acid Phosphatase, Leukocyte (TRAP) Kit according to manufacturer's instructions (Sigma-Aldrich). For *in situ* hybridization analyses, sections were hybridized to DIG-labeled RNA probes for detection of RNA transcripts. Sections were treated with 10µg/mL of proteinase K and acetylated prior to hybridization with probe. DIG-labeled RNA probes were synthesized from plasmids containing full-length cDNA or fragments of *Ctsk* and *Acp5*. *In situ* hybridization analyses were performed using standard protocols and previously performed *in situ* hybridizations were also referenced (genepaint.org) [21] (Figure 3).

Micro-computed tomography (MicroCT)

Specimens were imaged at the Small Animal Tomographic Analysis (SANTA) facility located at the Seattle Children's Research Institute using a Skyscan 1076 micro-Computed Tomograph (microCT). Scans were done at an isotropic resolution of 17.21µm using the following settings: 55kV, 179µA, 0.5mm Aluminum filter, 460ms exposure, rotation step of 0.7°, 180° scan, and 3 frame averaging. All data were reconstructed using Nrecon (Version 1.6.9.4) with the same greyscale threshold. Reconstructions were converted to 3D volumes using Drishti v2.4 [22] (Figure 6).

Statistics

Statistical analysis was performed on osteoclast quantification and linear measurements using the one-way Anova test in Stata version 12.0 (STATA Corp., Texas, USA).

Software

MicroCT data were retrieved using Amira analysis software (v5.4.2; FEI Inc.). Linear measurements from 3D-reconstructed microCT scans were made on the mouse mandibles from condylion to gonion, condylion to pogonion, and from pogonion to gonion. Measurements of the posterior cranial base bones, the basioccipital and the basisphenoid were also measured. Using the anterior and posterior boarder of the basioccipital and the basisphenoid bones we are able to compare both alendronate treatment and the *Ctsk*^{Cre};DTA^{fl/+} phenotype to see if the mandible is affected to a greater or lesser extent compared with other craniofacial bones. The posterior portion of the basioccipital will be identified as basion (Ba) and the anterior portion as occipitus (Occ). The anterior portion of basisphenoid will also be established as Occ and the anterior portion as sella (S).

The most anterior and posterior points of each mouse skull was used to determine the length size of the skull so that linear measurements could be adjusted for overall size of each individual animal.

Corrected linear measurements were calculated by first determining which subject had the smallest anterior posterior length of the skull and then calculating by what percent larger, other subject skulls were. Measurements were divided by these percentages to get the corrected

linear measurement values. Percent compared with control values were calculated by averaging the corrected linear measurements of control animals and setting this value as 100%. Average values of experimental mice were compared with controls and expressed as a percentage relative to control values.

Results:

Analyses of mice treated with alendronate *in utero* at E12.5 and $Ctsk^{Cre};DTA^{fl/+}$ mice

To investigate the role of osteoclasts and their activity, we injected alendronate *in utero* at E12.5 and analyzed the offspring at 3 months of age. $Ctsk^{Cre};DTA^{fl/+}$ were also analyzed at 3 months. We noted a difference in osteoclast number between control and $Ctsk^{Cre};DTA^{fl/+}$ samples (Figure 5). Control samples showed an average of 269.5 osteoclasts per sample whereas $Ctsk^{Cre};DTA^{fl/+}$ samples showed 1043.25 osteoclasts on average. $Ctsk^{Cre};DTA^{fl/+}$ samples had a greater range of osteoclasts present, the highest being 2133 and the lowest being 413 TRAP positive cells (Figure 5). Samples of alendronate-treated mice were not obtained for analysis.

Macroscopic evaluation was performed on microCTs of mouse skulls. Gross morphology, size, and shape of the samples skull and jaw bones were similar overall. One $Ctsk^{Cre};DTA^{fl/+}$ male did display some anatomical abnormalities. This mouse possessed a shortened nasal bone, shorter maxillary incisors that also did not curve inferiorly like other samples, and diastemas between upper and lower incisors (Figure 7). The anatomical abnormalities of this mouse were limited to the incisors and anterior, superior portion of the craniofacial complex. The superior, inferior, and oblique views of the $Ctsk^{Cre};DTA^{fl/+}$ and control mice showed incisors meeting edge-to-edge or with minimal overjet (Figure 8). Alendronate-treated mice did not display any gross morphological differences compared with controls (Figure 8). $Ctsk^{Cre};DTA^{fl/+}$ males and females appeared to on average have slightly larger overjets compared with control and alendronate-treated males and females (Figure 8)

Measurements of mouse skulls

Linear measurements of mouse skull microCT landmarks performed in Amira (v5.4.2; FEI Inc.) yielded minor variances between alendronate-treated, *Ctsk*^{Cre};DTA^{fl/+} and control animals (Figures 10-19). To note, condylion (Co) to pogonion (Pg) and gonion (Go) to Pg are sagittal jaw measurements.

Alendronate treatment did not affect the Co to Pg length in females. However, the males treated with alendronate had Co-Pg length increased by 0.22mm or 1.037 percent increase on average (Figure 10). The opposite was observed in *Ctsk*^{Cre};DTA^{fl/+} mice (Figure 15). *Ctsk*^{Cre};DTA^{fl/+} males and females had an Co-Pg length of 10.05mm compared with 10.37mm of control subjects. This is a 4% decrease overall. The female *Ctsk*^{Cre};DTA^{fl/+} Co-Pg length was 0.564mm shorter, or 5.5% less compared with female controls.

Both male and female alendronate-treated mice displayed a distinct trend of longer Go – Pg lengths when compared to controls (Figure 12). Male mice exposed to alendronate had Go – Pg measurement on average 0.1mm longer and females exposed to alendronate had Go – Pg lengths 0.732mm longer. This translates into 1.03 and 7.7 percent longer respectively, and is statistically significant with $p \leq 0.032514$. It should be noted that the large increase observed in females was due to the female controls having a shorter Go – Pg on average compared with the average of male controls. *Ctsk*^{Cre};DTA^{fl/+} males and females had shorter Go – Pg measurements compared with controls (Figure 17). With all subjects compared, the length of Go – Pg was 1.59mm or 8.87% shorter in *Ctsk*^{Cre};DTA^{fl/+} mice. The Go – Pg in *Ctsk*^{Cre};DTA^{fl/+} males and females measured 0.649mm and 3.49mm shorter respectively. In percentage terms, this is 4.28% and 18.03% shorter when compared with sex-matched controls. With the sexes pooled, the

difference between $Ctsk^{Cre};DTA^{fl/+}$ and control mice was nearly significant with $p \leq 0.056749$. Males alone were not significantly different and statistics could not be run for females alone due to sample size.

Co - Go length is a vertical measurement of the posterior portion of the mandible. Linear measurements of Co - Go were very consistent between alendronate-treated and control mice (Figure 11). There was less than 0.01mm difference when males and females were pooled together. The males showed the greatest change with 0.036mm or 0.8% longer with alendronate treatment. $Ctsk^{Cre};DTA^{fl/+}$ mice had shorter Co - Go measurements when compared to controls (Figure 16). Male and female $Ctsk^{Cre};DTA^{fl/+}$ Co - Go were 0.53mm, or 7.25% shorter compared to the average of control mice. Due to the variability between samples, this value was not significant with $p \leq 0.113166$. There was a large difference between controls and $Ctsk^{Cre};DTA^{fl/+}$ Co - Go lengths. The lone $Ctsk^{Cre};DTA^{fl/+}$ females was 1.57mm shorter, a 19.29% difference compared with controls. Once again, a p value could not be assigned due to limited specimen number.

Alendronate-treated and control mice exhibited no significant differences in the posterior cranial base measurement Ba - Occ (Figure 13). The pooled male and female samples were only 0.61% larger on average compared with controls. Neither the male or female animals differed from sex-matched controls. $Ctsk^{Cre};DTA^{fl/+}$ mice did display a slightly reduced Ba - Occ length compared to controls (Figure 18). This measurement was 0.06mm or 2.16% shorter in $Ctsk^{Cre};DTA^{fl/+}$ mice.

The second cranial base measurement Occ - S (sella) was slightly increased in the alendronate-treated mice at 0.04mm or 1.3% longer (Figure 14). This increase was a result of the

male samples as the female alendronate-treated mice had the same measurements as controls. Occ – S was slightly reduced in *Ctsk*^{Cre};DTA^{fl/+} mice by 2.07% (Figure 19). Males alone possessed Occ – S lengths 0.15mm or 3.65% shorter compared to controls. Occ – S in *Ctsk*^{Cre};DTA^{fl/+} female mice was the one measurement that was larger compared with the female controls. *Ctsk*^{Cre};DTA^{fl/+} females had Occ – S measurements 0.089mm or 1.09% longer.

Discussion

To test the hypothesis that inhibiting osteoclasts and their activity leads to mandibular prognathism commonly observed in human Class III skeletal malocclusions, we attempted to inhibit osteoclasts using 2 distinct methods: injection of alendronate *in utero* at E12.5 and generation of $Ctsk^{Cre};DTA^{fl/+}$ mice. With alendronate treatment, osteoclasts have the ability to resorb bone normally. However, once osteoclasts start to resorb bone, they are exposed to alendronate, which causes inhibition of the HMG-CoA reductase pathway leading to a breakdown of the actin cytoskeleton, decreased cell mobility and adhesion, and cell death [12]. $Ctsk^{Cre};DTA^{fl/+}$ mice harbor osteoclasts that function in resorbing bone normally as they have one copy of wildtype *Ctsk* [23, 24]. Osteoclasts will become mature and start the resorption process once they are stimulated by RANKL [25, 26]. This maturation includes expression activation of the *Ctsk* promoter, which in $Ctsk^{Cre};DTA^{fl/+}$ mice will cause expression of DTA and result in cell death [20]. In both models, osteoclasts will initiate bone resorption but the process will be halted by cell death.

Surprisingly, we noted an increase in TRAP-positive cells in $Ctsk^{Cre};DTA^{fl/+}$ mice indicating an increased number of osteoclasts and/or osteoclast activity compared to controls. This outcome was observed previously and is consistent with findings by another group [27]. The reason for increased TRAP staining in $Ctsk^{Cre};DTA^{fl/+}$ mice is unclear but it is possible that *Ctsk* expression is intricately involved in the regulation of osteoclast proliferation, maturation, or recruitment [27]. The variability of TRAP positive cells suggests that the increase in cell number may be transient or vary greatly in different areas due to different levels of bone maturation. TRAP staining in alendronate samples was performed in 6-week old mice but we did not observe any difference compared to controls (data not shown). This suggests that osteoclasts are

transiently inhibited when alendronate is injected at E12.5 although differences in TRAP staining still remain to be determined. Towards this end, we plan to inject alendronate at E12.5 and assay for TRAP activity at E16.5.

The gross morphology of the experimental and control mouse skulls revealed no noticeable differences in the alendronate experiments. Our protocol of injecting 1mg/kg of alendronate was based on previous work in avian systems where a significant outcome was observed [1]. However, 1mg/kg dose may not be sufficient in mammalian systems to achieve similar outcomes in lower jaw lengths. We even believed it to be on the higher end to what many groups were exposing experimental mice [28]. However, increasing either the dose or the number of alendronate administrations may have a more robust effect in the determination of mouse jaw lengths [29, 30]. We plan to continue our studies by altering the dosage amount and number since there were slight trends towards longer and shorter mandibles in alendronate-treated mice and *Ctsk*^{Cre};DTA^{fl/+} mice, respectively.

Ctsk^{Cre};DTA^{fl/+} mice exhibited increased overjets and more retrognathic mandibles on average, which would be consistent with an increase in osteoclasts and their activity. Other gross morphological features were the same as controls except for the one male subject mentioned earlier. Since only the one mouse skull was available for examination and measurements we cannot determine whether other anatomical anomalies were present. However, this mouse may have been exhibiting a murine version of Pycnodysostosis, also known as Toulouse-Lautrec Syndrome. An individual with pycnodysostosis will present with osteopetrosis, short stature, and delays in cranial suture closure [31, 32]. Other craniofacial abnormalities such as irregular teeth and midface deficiencies can be present [32]. Additional *Ctsk*^{Cre};DTA^{fl/+} male mice will need to be evaluated to determine the prevalence and extent of these anatomical abnormalities.

The Co – Pg and Go – Pg sagittal mandible measurements showed a slight but consistent trend of being longer in alendronate-treated animals. This result is consistent with previous work in quails and further supports that osteoclast activity and bone resorption inhibition will lead to a more prognathic mandible. Neither the cranial base bones nor the vertical height of the mandible was different compared with control samples. This suggests that alendronate treatment may have more of an effect in the anterior and middle portion of the mandible as changing the growth of the condyle in the posterior would affect the vertical height of the mandible. Future experiments with varying doses and times may help solidify these minor trends observed in this study.

Besides the Occ – S measurement in females, all of the linear measurements made in *Ctsk*^{Cre};DTA^{fl/+} mice were shorter compared to controls. The difference was as great as 19.29% shorter suggesting that altering bone resorption can have a remarkable effect on the size of craniofacial bones. Greater differences compared with controls were seen in the mandibular measurements supporting the results observed in avian experiments [1]. Despite the gross morphological differences observed in the one *Ctsk*^{Cre};DTA^{fl/+} mouse, the linear measurements were very similar to the other male sample that did not have the observable abnormalities. Our sample size of *Ctsk*^{Cre};DTA^{fl/+} mice was limited and did not allow us to run statistics on individual sexes. The most significant difference measured was Go – Pg at 8.87% smaller in *Ctsk*^{Cre};DTA^{fl/+} compared to controls ($p \leq 0.066801$). Additional *Ctsk*^{Cre};DTA^{fl/+} mice will be generated for further future experiments.

The opposing trends observed in the alendronate and *Ctsk*^{Cre};DTA^{fl/+} groups are interesting but consistent. Since osteoclasts are the targeted cells in both models, we hypothesized the same result from both. *CTSK* mutations in humans cause shorter long bones, which is consistent with our findings in this study [31, 32]. While the *CTSK* gene is fairly

specific for osteoclasts, it is also expressed in heart tissue during development, skeletal muscle, cartilage, breast cancer cells, and osteocytes derived from stem cells [33-35]. With these other tissue and cell types being affected by *CTSK* downregulation, it is possible that the shorter measurements are a result of osteocyte inhibition in addition to osteoclasts being affected.

Future experiments will provide insight into how bone metabolism affects jaw growth. Beyond completing analyses of additional alendronate-treated and *Ctsk*^{Cre};DTA^{fl/+} mice, TRAP staining in E18.5 mice treated with alendronate at E12.5 and varying dosages of alendronate treatment, high calcium and low phosphorus conditions have previously been shown to lead to osteoclast inhibition [36-38]. Therefore, a diet high in calcium and low in phosphorus during pregnancy may be associated in the development of class III skeletal malocclusions in the offspring of specific populations. To test this hypothesis, mice will be maintained on high calcium, low phosphorus diets and their craniofacial bones analyzed.

Conclusion:

The results from this study indicate that altering osteoclasts (e.g., number and activity) may have an effect on the development of the mammalian mandible, in particular in the sagittal dimension. Specifically, inhibition of osteoclasts led to longer mandibles, whereas activation of osteoclasts led to shorter mandibles. Additional experiments are required to support and strengthen our finding. We will perform further experiments varying the dosage of alendronate (e.g., number of injections and concentration), as well as increasing the number of specimens for both alendronate-treated and *Ctsk*^{Cre};DTA^{fl/+} mice. Our data presented here lays the foundation for better understanding the role of bone metabolism in the development of the mandible and skeletal jaw relationships. With this knowledge, we hope to one day predict and ultimately, prevent the development of skeletal malocclusions.

References

1. Ealba, E.L., et al., *Neural crest-mediated bone resorption is a determinant of species-specific jaw length*. Dev Biol, 2015. **408**(1): p. 151-63.
2. Graber, L.W., R.L. Vanarsdall, and K.W.L. Vig, *Orthodontics : current principles & techniques*. 2012, Philadelphia, PA: Elsevier/Mosby.
3. Proffit, W.R., H.W. Fields, Jr., and D.M. Sarver. *Contemporary Orthodontics*. 2014; Available from: <http://public.eblib.com/choice/publicfullrecord.aspx?p=2072311>.
4. Posnick, J.C., 3 - *Definition and Prevalence of Dentofacial Deformities*, in *Orthognathic Surgery*, J.C. Posnick, Editor. 2014, W.B. Saunders: St. Louis. p. 61-68.
5. Angle, E.H., *Treatment of malocclusion of the teeth : Angle's system*. 1907, Philadelphia: White Dental Manufacturing Co.
6. Joshi, N., A.M. Hamdan, and W.D. Fakhouri, *Skeletal malocclusion: a developmental disorder with a life-long morbidity*. J Clin Med Res, 2014. **6**(6): p. 399-408.
7. Carlson, D.S., *Evolving concepts of heredity and genetics in orthodontics*. Am J Orthod Dentofacial Orthop, 2015. **148**(6): p. 922-38.
8. da Fontoura, C.S., et al., *Candidate Gene Analyses of Skeletal Variation in Malocclusion*. J Dent Res, 2015. **94**(7): p. 913-20.
9. Perillo, L., et al., *Genetic association of ARHGAP21 gene variant with mandibular prognathism*. J Dent Res, 2015. **94**(4): p. 569-76.
10. Ikuno, K., et al., *Microsatellite genome-wide association study for mandibular prognathism*. Am J Orthod Dentofacial Orthop, 2014. **145**(6): p. 757-62.
11. Jang, J.Y., et al., *Polymorphisms in the Matrilin-1 gene and risk of mandibular prognathism in Koreans*. J Dent Res, 2010. **89**(11): p. 1203-7.
12. Cozin, M., et al., *Novel therapy to reverse the cellular effects of bisphosphonates on primary human oral fibroblasts*. J Oral Maxillofac Surg, 2011. **69**(10): p. 2564-78.
13. Alfaqeeh, S., et al., *Root and Eruption Defects in c-Fos Mice Are Driven by Loss of Osteoclasts*. Journal of Dental Research, 2015. **94**(12): p. 1724-1731.
14. Xue, F., R.W. Wong, and A.B. Rabie, *Genes, genetics, and Class III malocclusion*. Orthod Craniofac Res, 2010. **13**(2): p. 69-74.
15. Xue, F., A.B. Rabie, and G. Luo, *Analysis of the association of COL2A1 and IGF-1 with mandibular prognathism in a Chinese population*. Orthod Craniofac Res, 2014. **17**(3): p. 144-9.
16. Bune, A.J., et al., *Mice lacking tartrate-resistant acid phosphatase (Acp 5) have disordered macrophage inflammatory responses and reduced clearance of the pathogen, Staphylococcus aureus*. Immunology, 2001. **102**(1): p. 103-13.
17. Sibille, J.C., K. Doi, and P. Aisen, *Hydroxyl Radical Formation and Iron-Binding Proteins - Stimulation by the Purple Acid-Phosphatases*. Journal of Biological Chemistry, 1987. **262**(1): p. 59-62.
18. Hayman, A.R. and T.M. Cox, *Purple Acid-Phosphatase of the Human Macrophage and Osteoclast - Characterization, Molecular-Properties, and Crystallization of the Recombinant Di-Iron-Oxo Protein Secreted by Baculovirus-Infected Insect Cells*. Journal of Biological Chemistry, 1994. **269**(2): p. 1294-1300.
19. Chiu, W.S., et al., *Transgenic mice that express Cre recombinase in osteoclasts*. Genesis, 2004. **39**(3): p. 178-85.

20. Wu, S., Y. Wu, and M.R. Capecchi, *Motoneurons and oligodendrocytes are sequentially generated from neural stem cells but do not appear to share common lineage-restricted progenitors in vivo*. *Development*, 2006. **133**(4): p. 581-90.
21. *Genepaint*. 2016 May 24th 2016 [cited 2016 June 5th 2016]; May 24th 2016:[Available from: <http://genepaint.org/Frameset.html>].
22. Limaye, A., *Drishti, A Volume Exploration and Presentation Tool*. *Developments in X-Ray Tomography Viii*, 2012. **8506**.
23. Saftig, P., et al., *Impaired osteoclastic bone resorption leads to osteopetrosis in cathepsin-K-deficient mice*. *Proceedings of the National Academy of Sciences of the United States of America*, 1998. **95**(23): p. 13453-13458.
24. Winkeler, C.L., et al., *Cathepsin K-Cre Causes Unexpected Germline Deletion of Genes in Mice*. *Plos One*, 2012. **7**(7).
25. Troen, B.R., *The regulation of cathepsin K gene expression*. *Skeletal Development and Remodeling in Health, Disease, and Aging*, 2006. **1068**: p. 165-172.
26. Bradaschia-Correa, V., M.M. Moreira, and V.E. Arana-Chavez, *Reduced RANKL expression impedes osteoclast activation and tooth eruption in alendronate-treated rats*. *Cell and Tissue Research*, 2013. **353**(1): p. 79-86.
27. Zhuo, Y., et al., *Inhibition of bone resorption by the cathepsin K inhibitor odanacatib is fully reversible*. *Bone*, 2014. **67**: p. 269-280.
28. Aspenberg, P., et al., *Targeting RANKL for reduction of bone loss around unstable implants: OPG-Fc compared to alendronate in a model for mechanically induced loosening*. *Bone*, 2011. **48**(2): p. 225-30.
29. Araujo, A.S., et al., *New methodology for evaluating osteoclastic activity induced by orthodontic load*. *Journal of Applied Oral Science*, 2015. **23**(1): p. 19-25.
30. Bradaschia-Correa, V., et al., *Effect of alendronate on endochondral ossification in mandibular condyles of growing rats*. *Eur J Histochem*, 2012. **56**(2): p. e24.
31. Gelb, B.D., et al., *Pycnodysostosis, a lysosomal disease caused by cathepsin K deficiency*. *Science*, 1996. **273**(5279): p. 1236-8.
32. Motyckova, G., et al., *Linking osteopetrosis end pycnodysostosis: Regulation of cathepsin K expression by the microphthalmia transcription factor family*. *Proceedings of the National Academy of Sciences of the United States of America*, 2001. **98**(10): p. 5798-5803.
33. *CTSK cathepsin K [Homo sapiens (human)]*. *Gene* [Website] 2016 May 26th 2016 [cited 2016 June 1st 2016]; *CTSK Gene*. Available from: <http://www.ncbi.nlm.nih.gov/gene/1513>.
34. Chia, L.Y., et al., *Isolation and gene expression of haematopoietic-cell-free preparations of highly purified murine osteocytes*. *Bone*, 2015. **72**: p. 34-42.
35. Rantakokko, J., et al., *Mouse cathepsin K: cDNA cloning and predominant expression of the gene in osteoclasts, and in some hypertrophying chondrocytes during mouse development*. *Febs Letters*, 1996. **393**(2-3): p. 307-313.
36. Kanatani, M., et al., *High extracellular calcium inhibits osteoclast-like cell formation by directly acting on the calcium-sensing receptor existing in osteoclast precursor cells*. *Biochem Biophys Res Commun*, 1999. **261**(1): p. 144-8.
37. Takeyama, S., et al., *Low calcium environment effects osteoprotegerin ligand/osteoclast differentiation factor*. *Biochem Biophys Res Commun*, 2000. **276**(2): p. 524-9.

38. Nishimura, M., et al., *Cytological properties of stromal cells derived from giant cell tumor of bone (GCTSC) which can induce osteoclast formation of human blood monocytes without cell to cell contact.* J Orthop Res, 2005. **23**(5): p. 979-87.

Figures

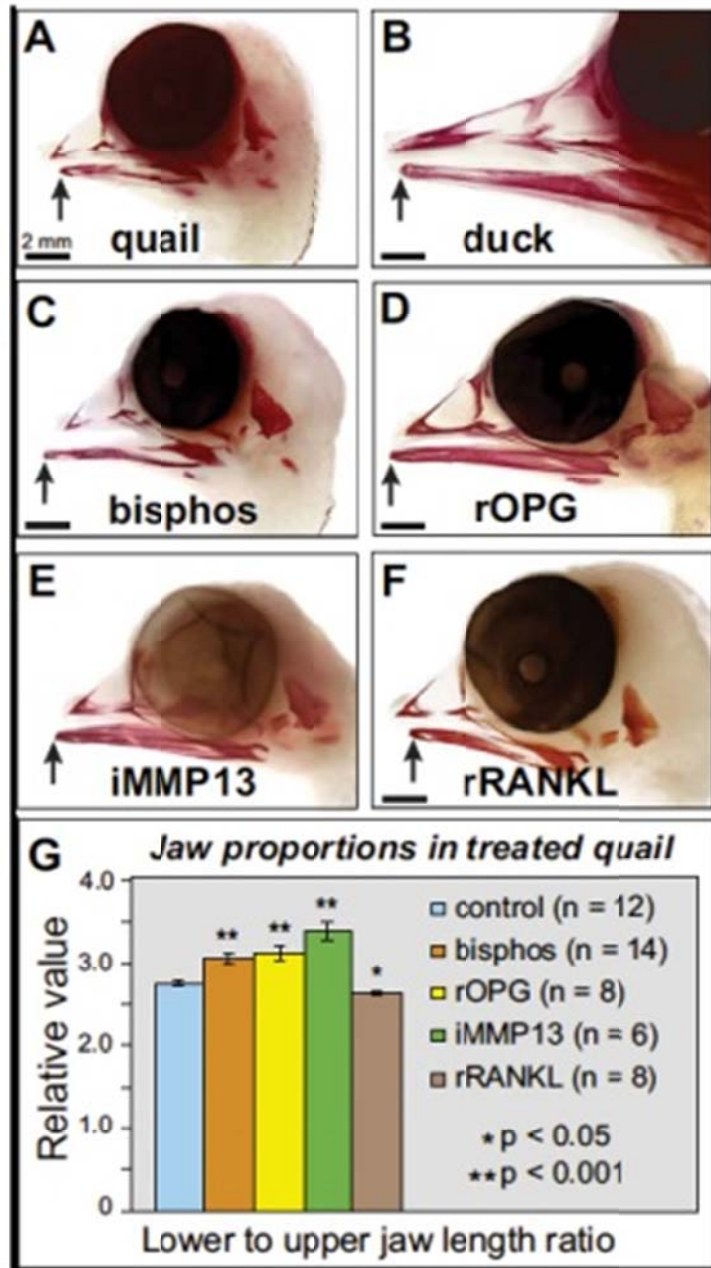


Figure 1. Bone resorption controls lower beak length [1].

(A-B) Beak skeletons at HH39 stained with alizarin red showing differences in length (arrows).

(C-F) Quail treated with the bisphosphonate alendronate (bisphos), recombinant OPG protein (rOPG), and an MMP13 inhibitor (iMMP13) resulted in longer lower beaks.

(F) rRANKL protein decreased lower beak length. (G) Quantifying beak size revealed significant treatment-dependent increases and decreases in beak lengths.



Figure 2. Mouse intraperitoneal injections.

The bisphosphonate alendronate (1mg/kg) for experimental mice and 0.9% saline for control mice was injected into pregnant mice at E12.5. The offspring were sacrificed at 3 months for analyses.

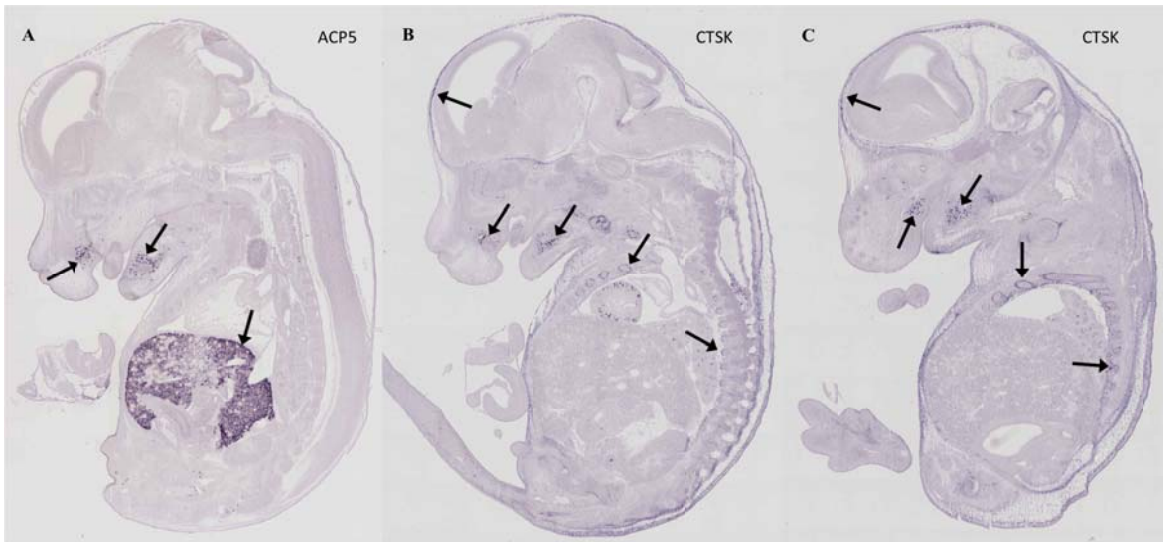


Figure 3. *In situ* hybridization of E14.5 mouse embryos [21] (genepaint.org).

A: *Acp5* mRNA, the gene that codes for TRAP is localized in the liver and incisor regions. B and C: *Ctsk* mRNA is expressed in the tooth developing regions, and areas of bone formation (ribs and cranium).

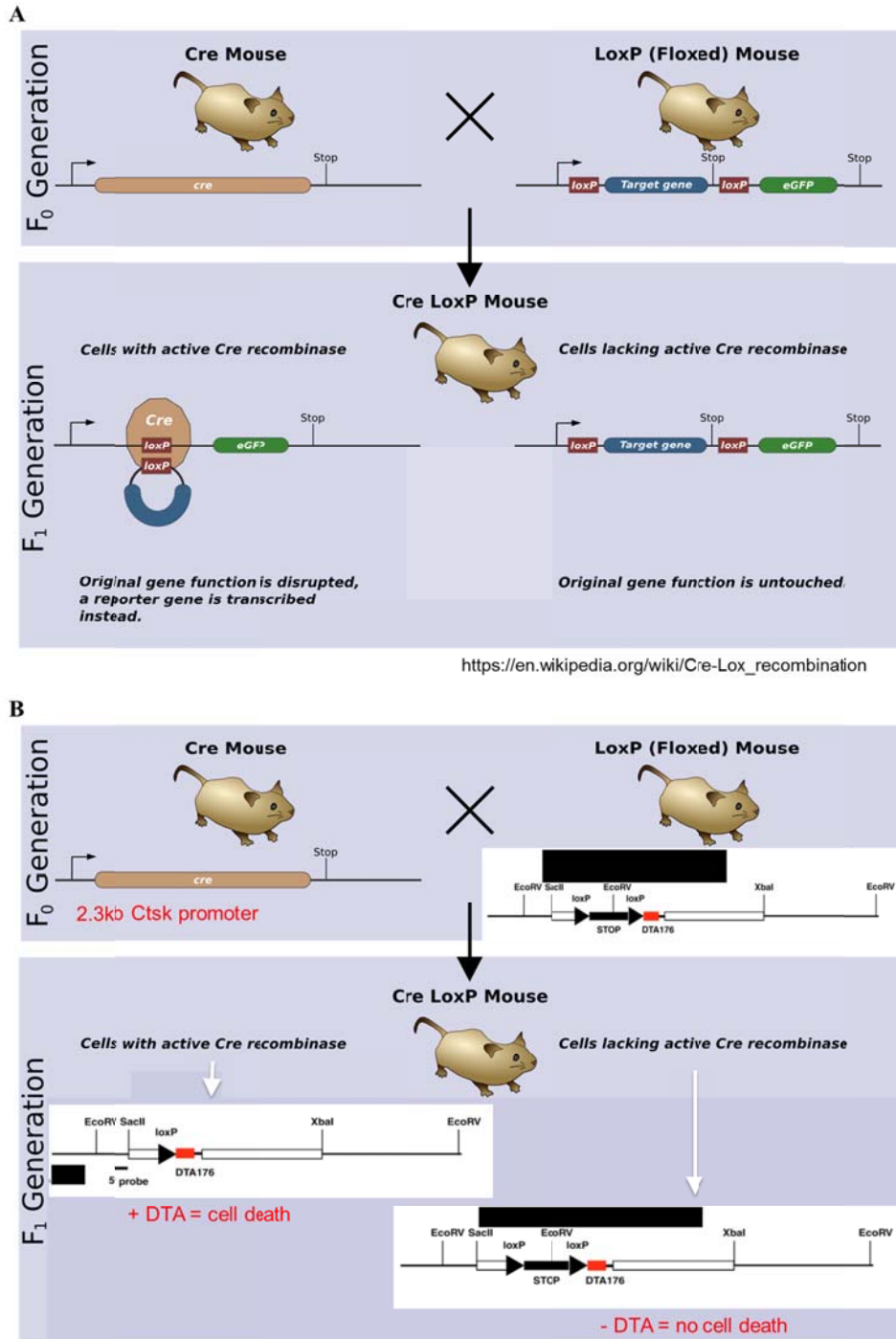


Figure 4. Generation of $Ctsk^{Cre};DTA^{fl/+}$ mice.

A) Cre recombinase is expressed under the control of a promoter from a gene of interest. When Cre recombinase is present, it will splice out the target gene through loxP sites. B) Cre recombinase is expressed under the *Ctsk* promoter leading the expression of DTA. The presence of DTA leads to cell death (e.g., osteoclasts).

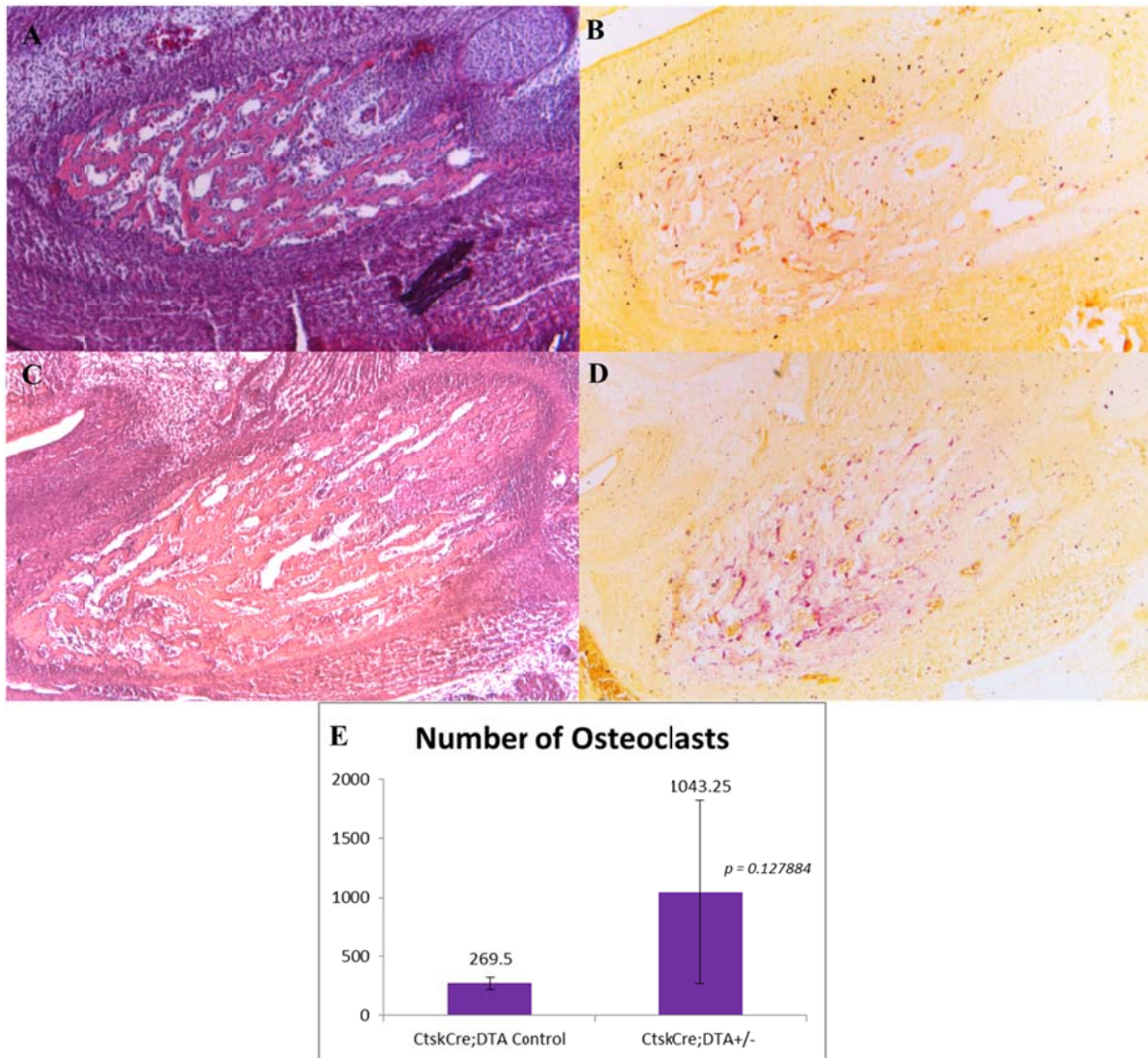


Figure 5. H&E and Tartrate-resistant acid phosphatase (TRAP) staining of mouse mandibular bone formation at E18.5. A) Control CTSK H&E B) Control CTSK TRAP staining displaying a normal number of osteoclasts. C) CTSK +/- H&E D) CTSK +/- TRAP staining displaying a significant increase of osteoclasts present compared with control.

A: *Ctsk*^{Cre};DTA Control E18.5 HE, 5X

B: *Ctsk*^{Cre};DTA Control E18.5 TRAP, 5X

C: *Ctsk*^{Cre};DTA^{fl/+} Mut E18.5 HE, 5X

D: *Ctsk*^{Cre};DTA^{fl/+} Mut E18.5 TRAP, 5X

E: TRAP staining summary of Control and *Ctsk*^{Cre};DTA^{fl/+} experimental mice

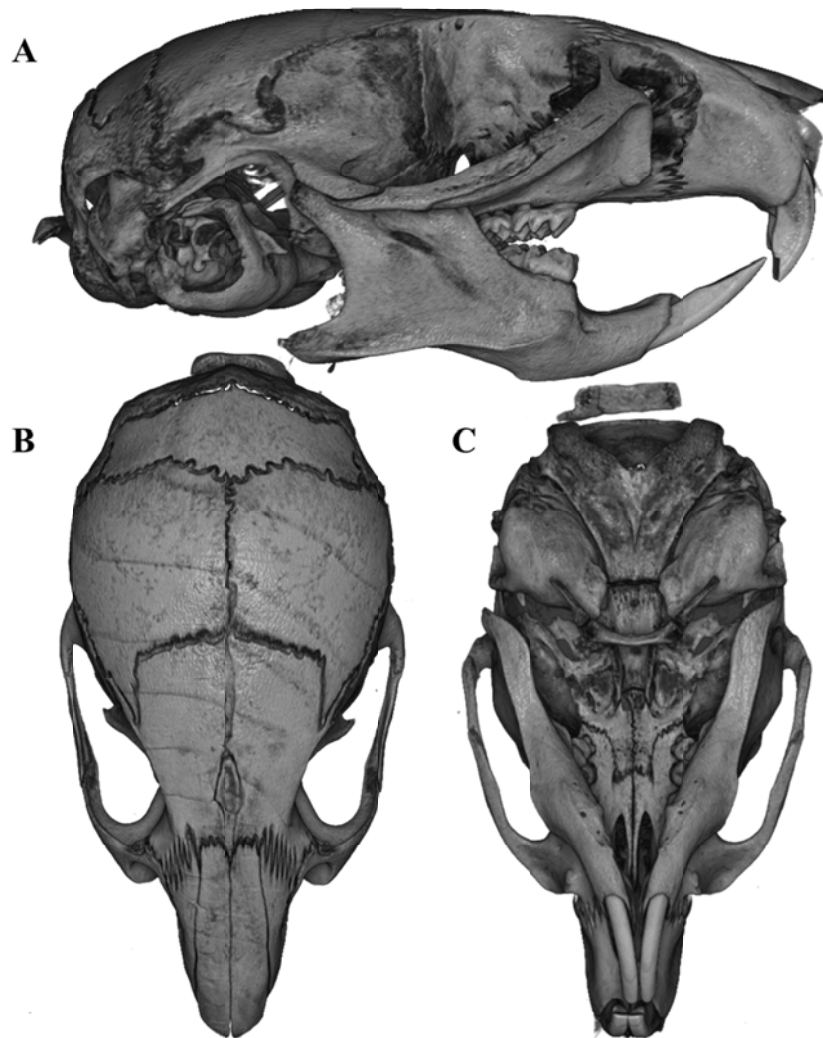


Figure 6. Detailed microCT reconstructions of a control male mouse skull.
A) Sagittal view B) Superior view C) Inferior view

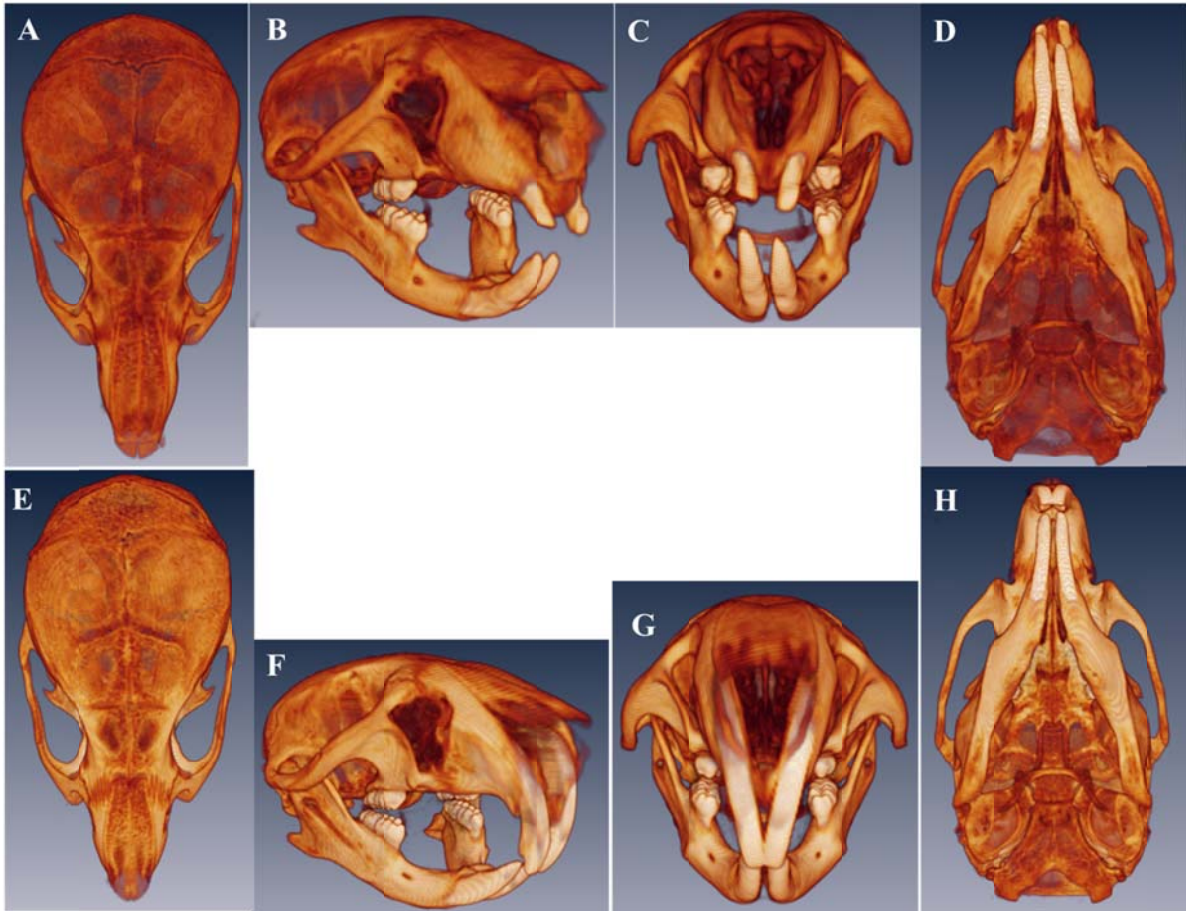


Figure 7. Morphometric comparison of control male and *Ctsk^{Cre};DTA^{fl/+}* male with anatomical abnormalities. *Ctsk^{Cre};DTA^{fl/+}* male (A-D) displays deviations of normal anatomy in the nasal bone and incisors compared with control male (E-H)



Figure 8. microCTs of mouse skull samples.

A = Control Male

B = Alendronate (1mg/kg) Male

C = Control Female

D = Alendronate (1mg/kg) Female

E = *Ctsk*^{Cre};DTA^{fl/+} Male Control

F = *Ctsk*^{Cre};DTA^{fl/+} Male

G = *Ctsk*^{Cre};DTA^{fl/+} Female Control

H = *Ctsk*^{Cre};DTA^{fl/+} Female



Figure 9 – Amira Landmarks

A) Sagittal view of a control male microCT skull with the landmarks used in this study to make linear measurements of the mandible. Pg (pogonion) is defined as the most anterior superior portion. Co (condylion) is the most superior point of the crest of the mandibular condyle. Go (gonion) is the most posterior point on the crest of the gonial angle.

B) Inferior view of a control male microCT skull with the landmarks used in this study to make linear measurements of the mandible. Ba (basion) is defined as the most posterior point of the midsagittal plane.

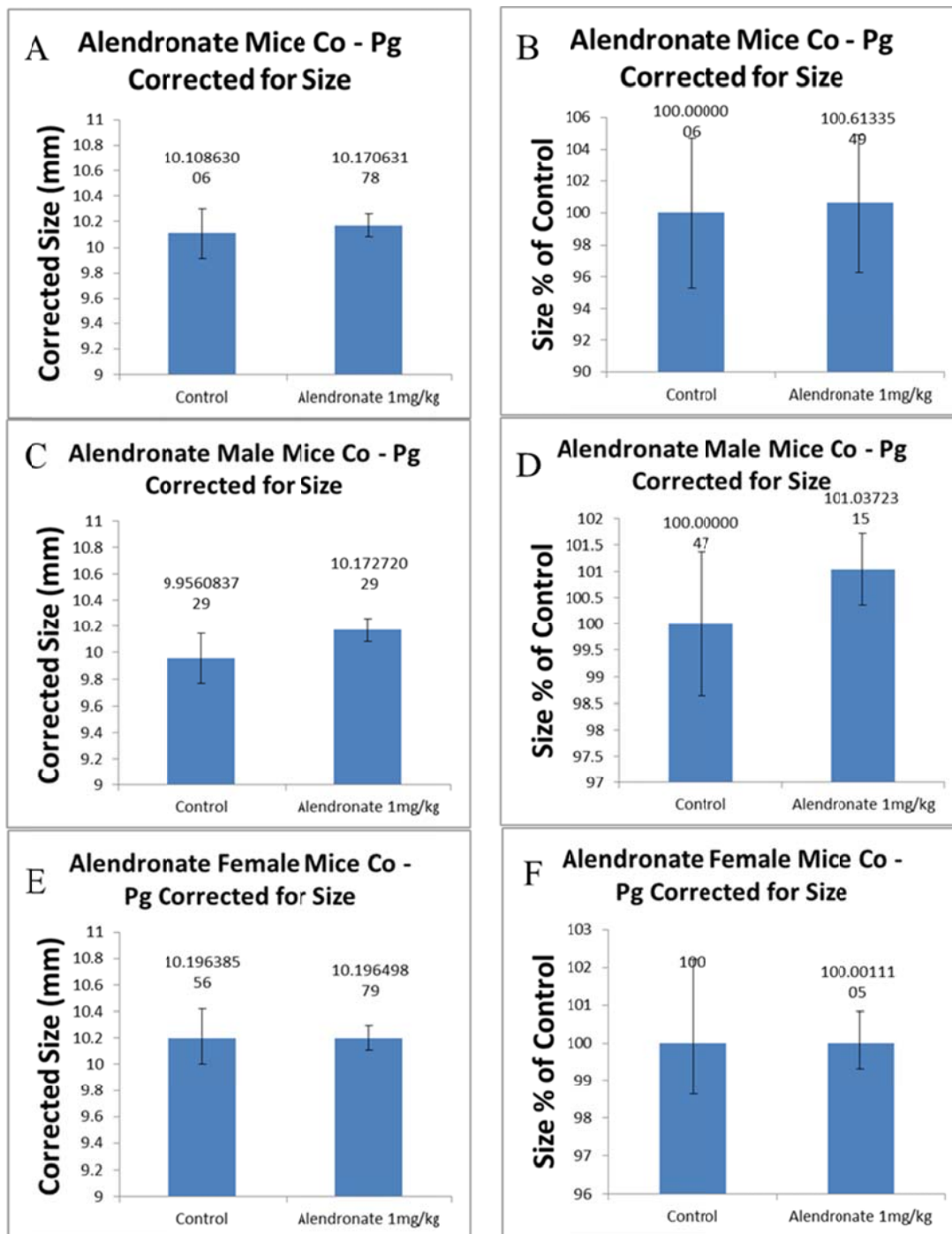


Figure 10. Sagittal Mn jaw measurement from Co to Pg in control and alendronate treated mice. A) Pooled males and females linear measurements. B) Measurements in A expressed as a percentage using control as 100%. C) Males linear measurements. D) Measurements in C expressed as a percentage using control as 100%. E) Females linear measurements. F) Measurements in E expressed as a percentage using control as 100%.

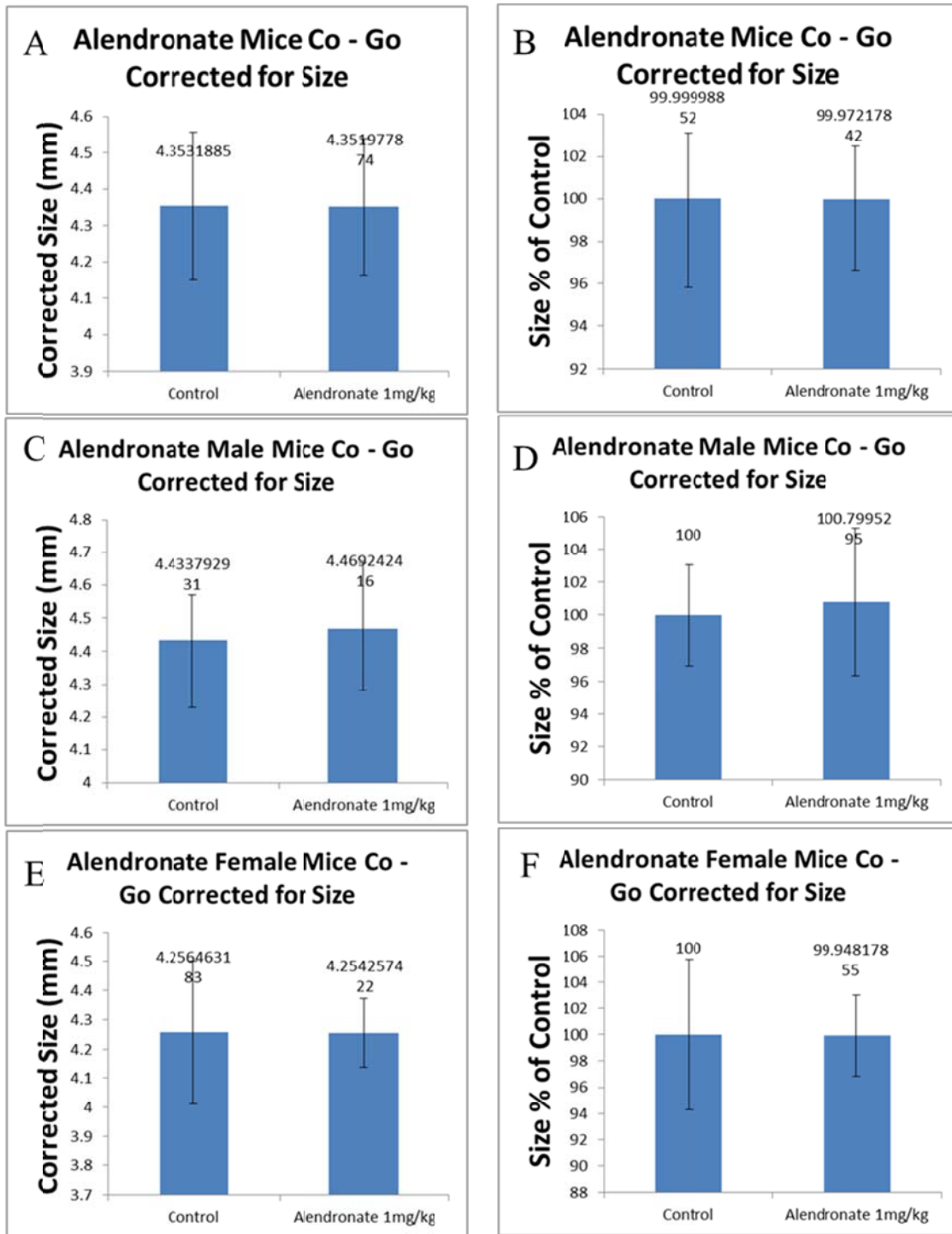


Figure 11. Vertical Mn jaw measurement from Co to Go in control and alendronate treated mice. A) Pooled males and females linear measurements. B) Measurements in A expressed as a percentage using control as 100%. C) Males linear measurements. D) Measurements in C expressed as a percentage using control as 100%. E) Females linear measurements. F) Measurements in E expressed as a percentage using control as 100%.

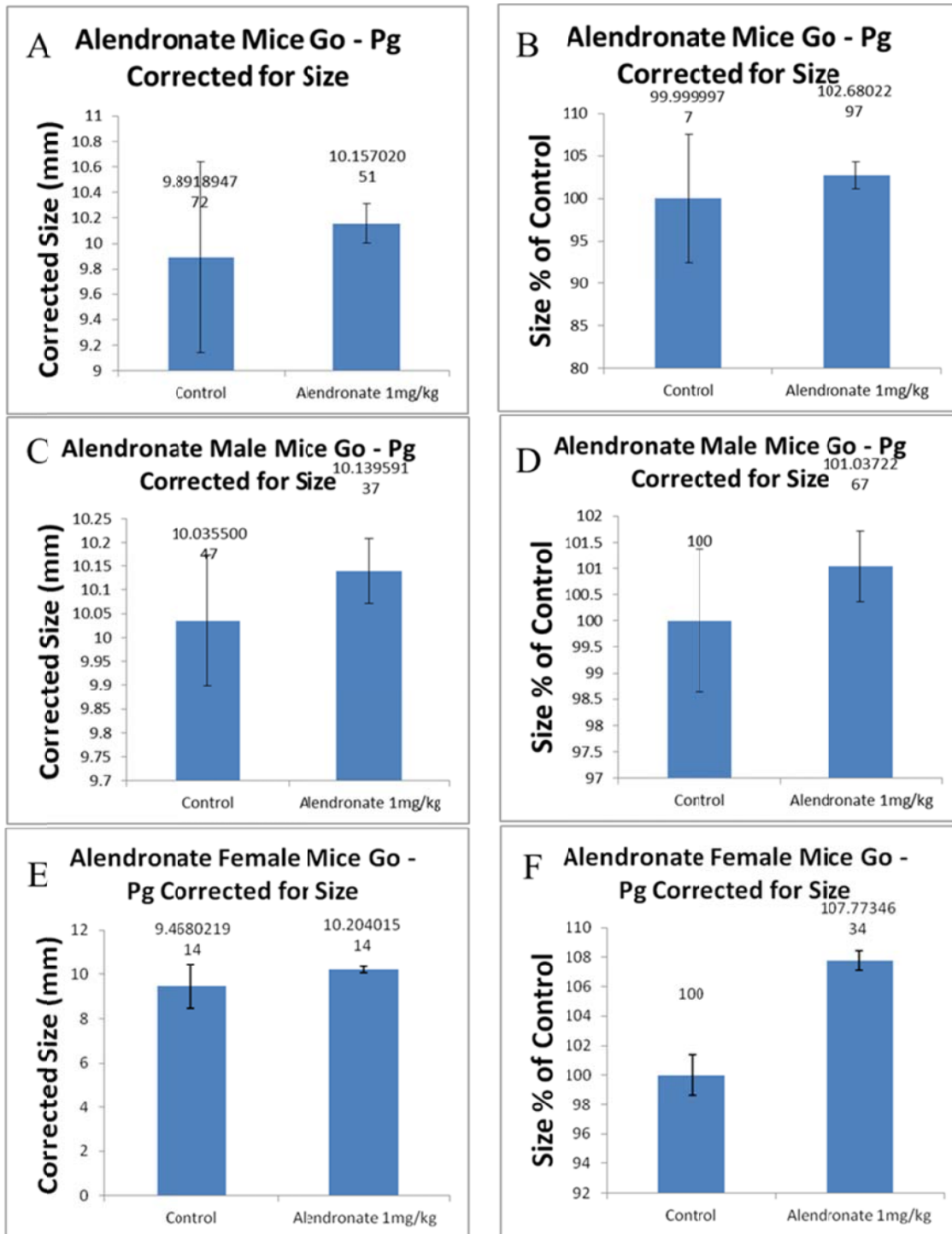


Figure 12. Sagittal Mn jaw measurement from Go to Pg in control and alendronate treated mice. A) Pooled males and females linear measurements. B) Measurements in A expressed as a percentage using control as 100%. C) Males linear measurements. D) Measurements in C expressed as a percentage using control as 100%. E) Females linear measurements. F) Measurements in E expressed as a percentage using control as 100%.

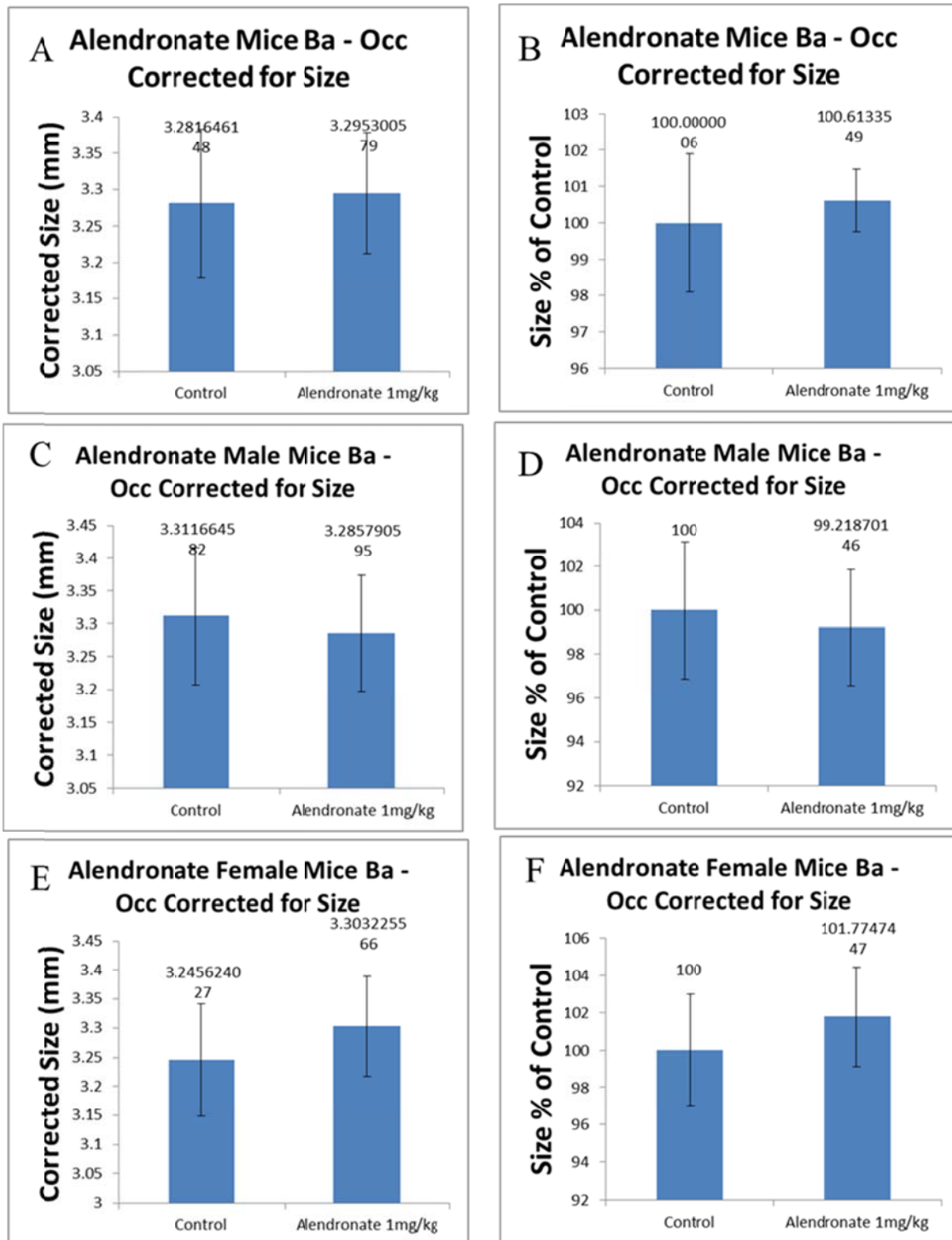


Figure 13. Cranial base measurement from Ba to Occ in control and alendronate treated mice. A) Pooled males and females linear measurements. B) Measurements in A expressed as a percentage using control as 100%. C) Males linear measurements. D) Measurements in C expressed as a percentage using control as 100%. E) Females linear measurements. F) Measurements in E expressed as a percentage using control as 100%.

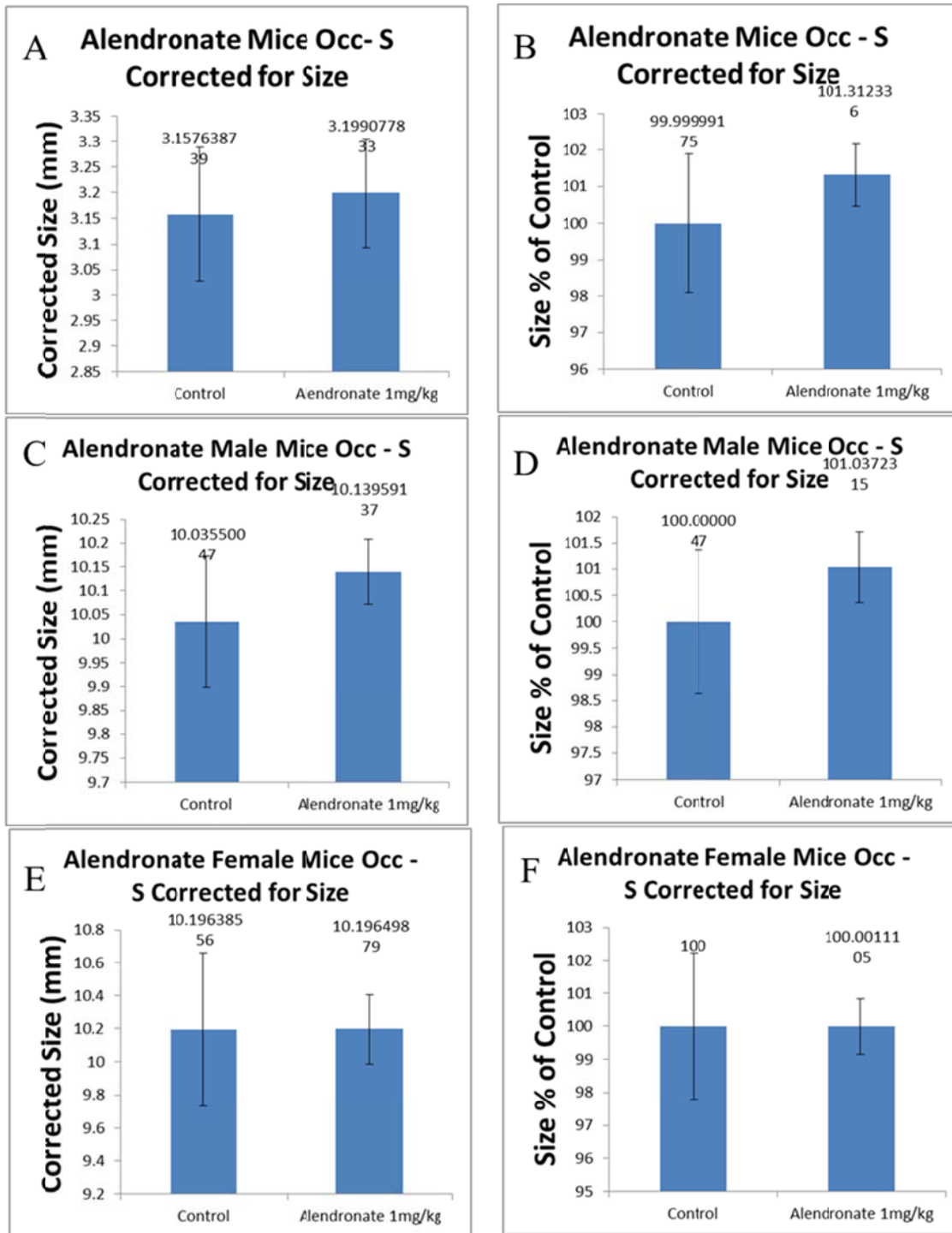


Figure 14. Cranial base measurement from Occ to S in control and alendronate treated mice. A) Pooled males and females linear measurements. B) Measurements in A expressed as a percentage using control as 100%. C) Males linear measurements. D) Measurements in C expressed as a percentage using control as 100%. E) Females linear measurements. F) Measurements in E expressed as a percentage using control as 100%.

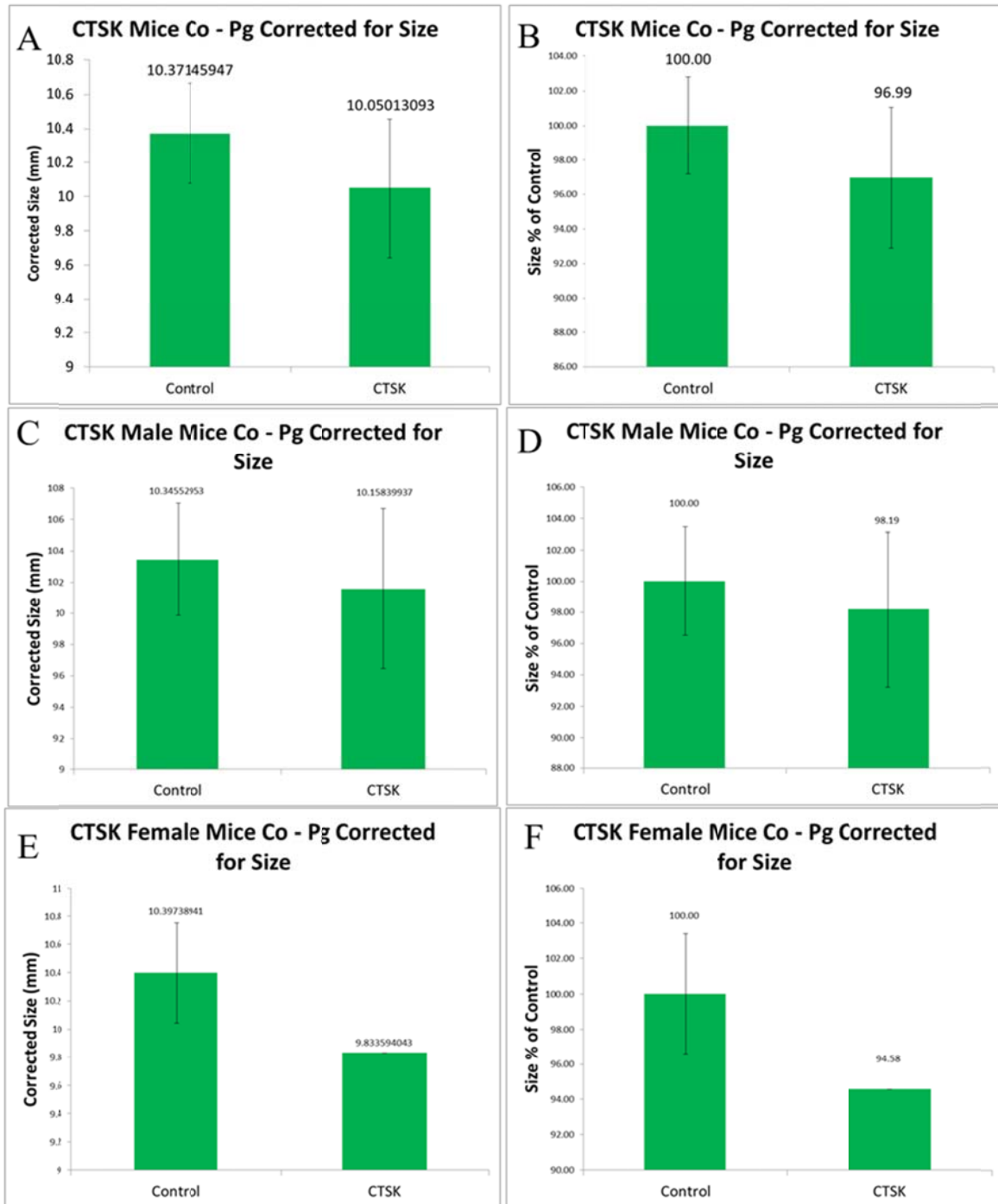


Figure 15. Sagittal Mn jaw measurement from Co to Pg in control and *Ctsk*^{Cre};DTA^{fl/+} mice. A) Pooled males and females linear measurements. B) Measurements in A expressed as a percentage using control as 100%. C) Males linear measurements. D) Measurements in C expressed as a percentage using control as 100%. E) Females linear measurements. F) Measurements in E expressed as a percentage using control as 100%. CTSK, *Ctsk*^{Cre};DTA^{fl/+}

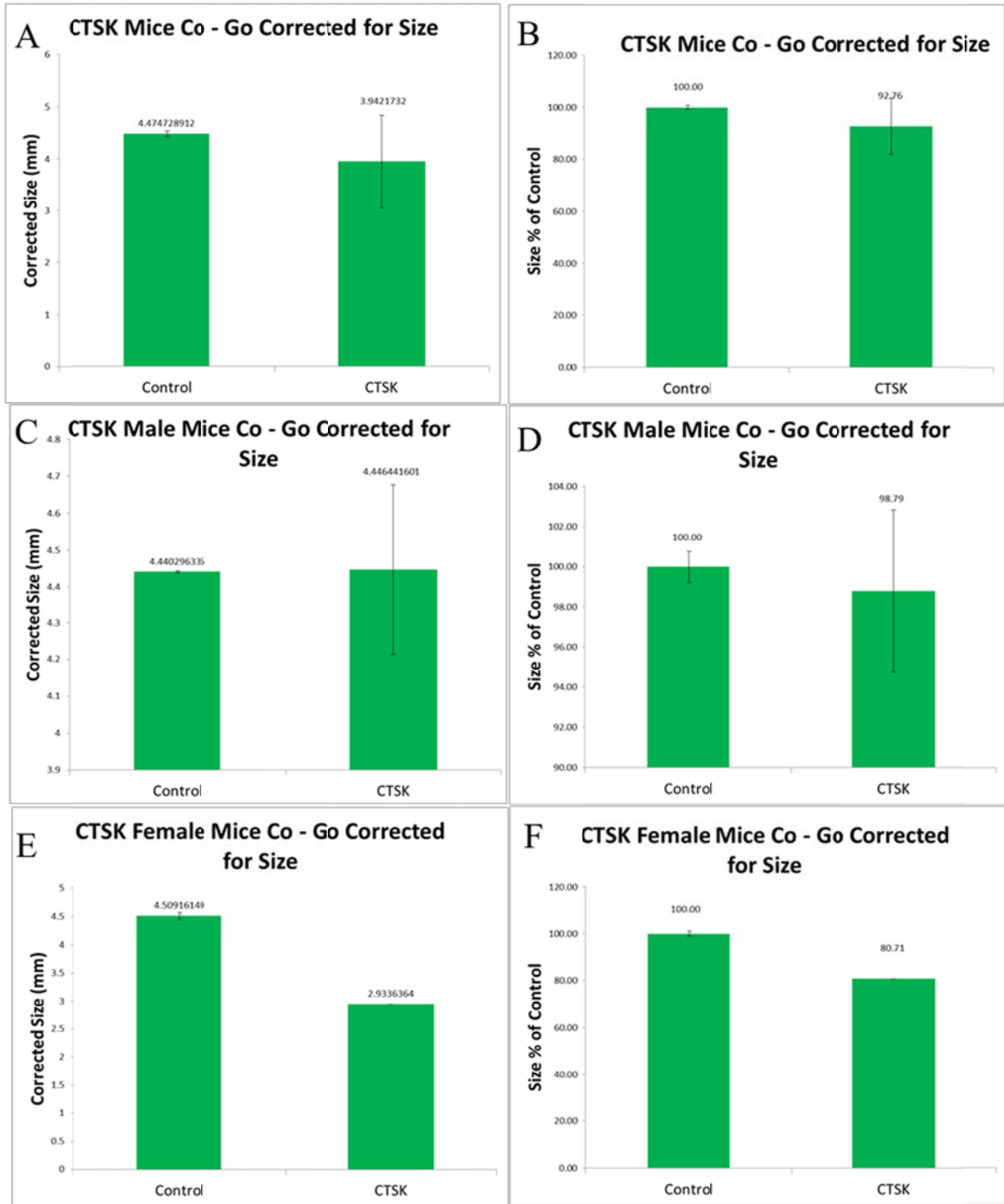


Figure 16. Vertical Mn jaw measurement from Co to Go in control and $Ctsk^{Cre};DTA^{fl/+}$ mice.

A) Pooled males and females linear measurements. B) Measurements in A expressed as a percentage using control as 100%. C) Males linear measurements. D) Measurements in C expressed as a percentage using control as 100%. E) Females linear measurements. F) Measurements in E expressed as a percentage using control as 100%. CTSK, $Ctsk^{Cre};DTA^{fl/+}$

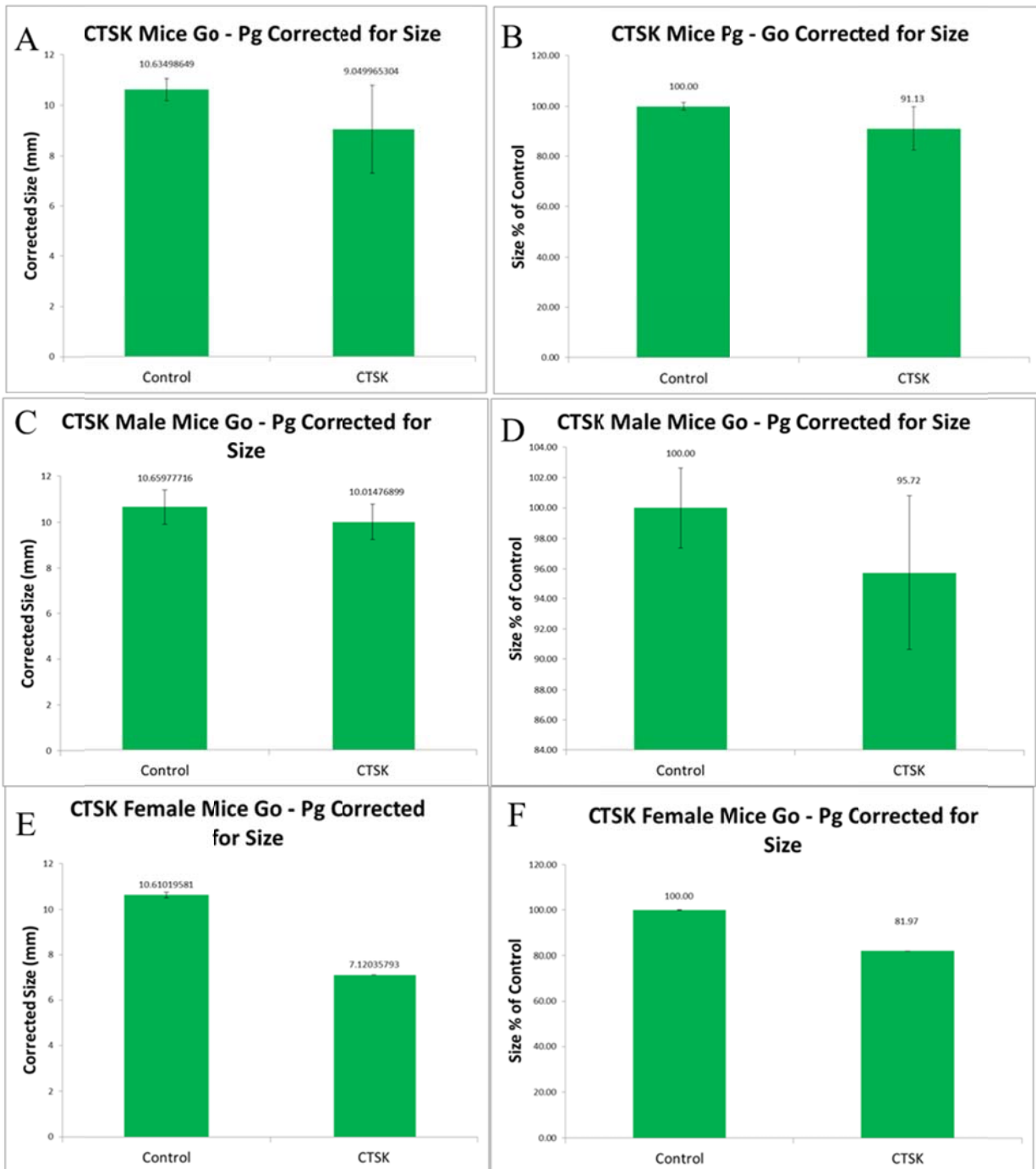


Figure 17. Sagittal Mn jaw measurement from Go to Pg in control and $Ctsk^{Cre};DTA^{fl/+}$ mice.

A) Pooled males and females linear measurements. B) Measurements in A expressed as a percentage using control as 100%. C) Males linear measurements. D) Measurements in C expressed as a percentage using control as 100%. E) Females linear measurements. F) Measurements in E expressed as a percentage using control as 100%. CTSK, $Ctsk^{Cre};DTA^{fl/+}$

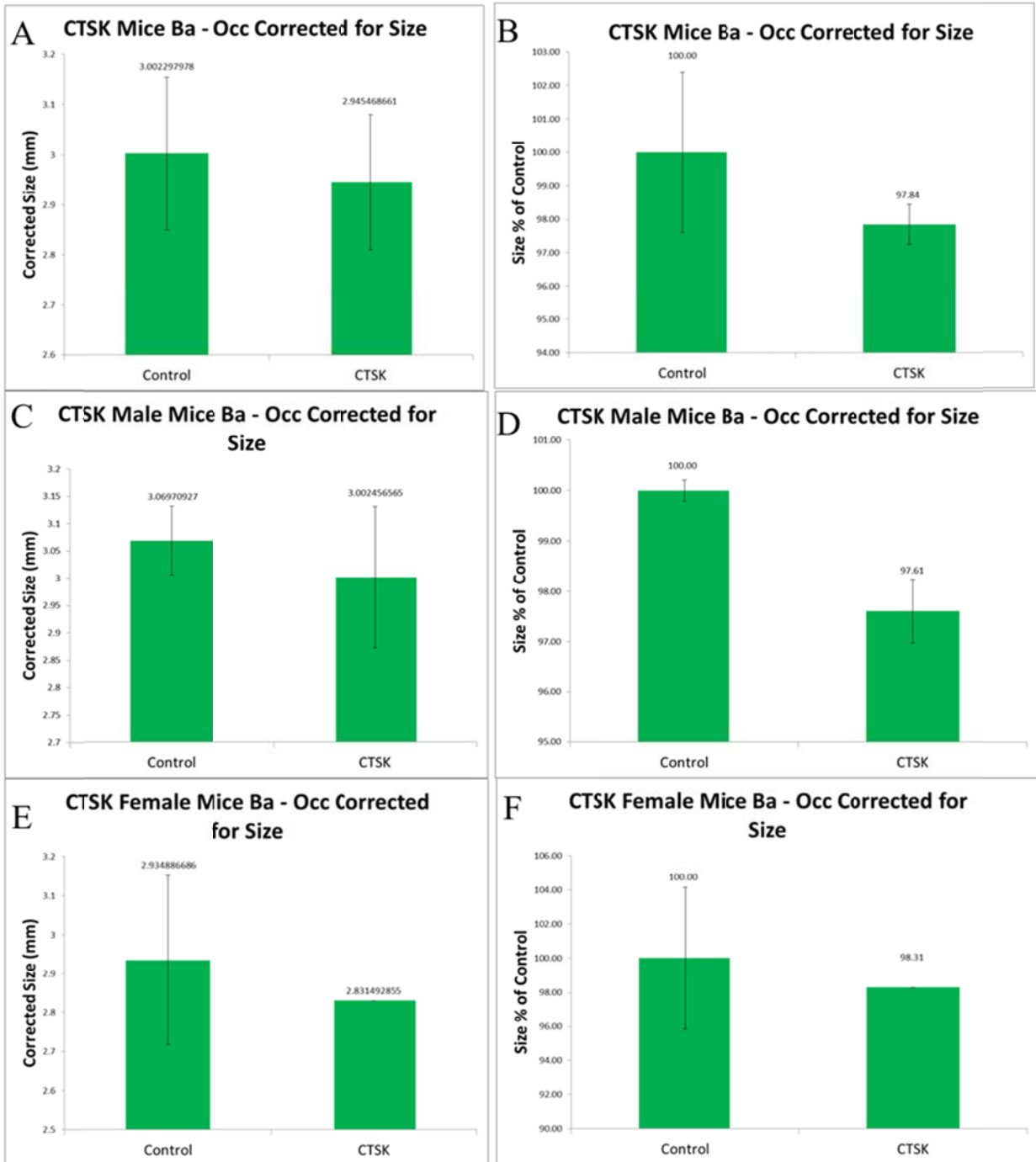


Figure 18. Cranial base measurement from Ba to Occ in control and $Ctsk^{Cre};DTA^{fl/+}$ mice. A) Pooled males and females linear measurements. B) Measurements in A expressed as a percentage using control as 100%. C) Males linear measurements. D) Measurements in C expressed as a percentage using control as 100%. E) Females linear measurements. F) Measurements in E expressed as a percentage using control as 100%. CTSK, $Ctsk^{Cre};DTA^{fl/+}$

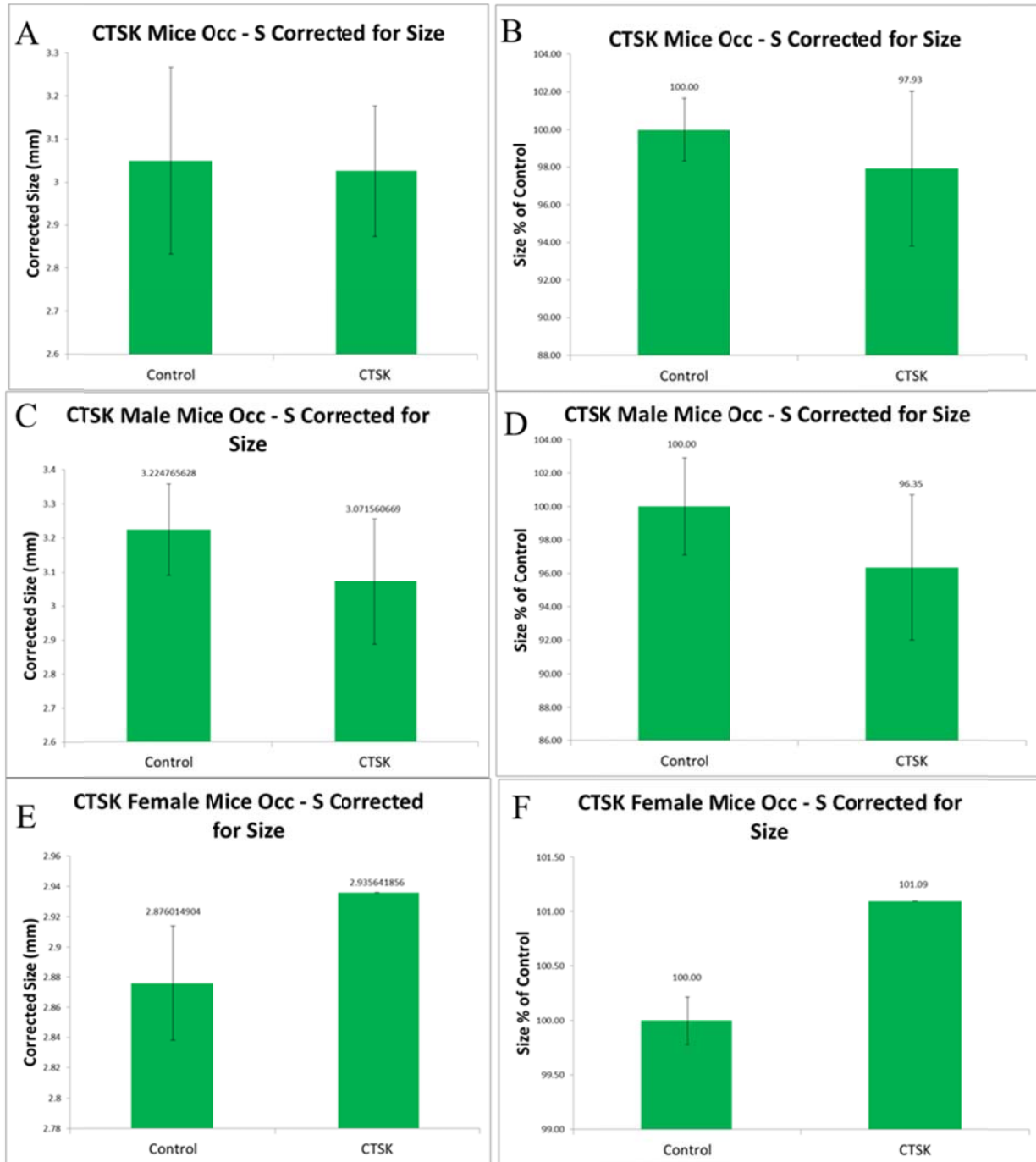


Figure 19. Cranial base measurement from Occ to S in control and $Ctsk^{Cre};DTA^{fl/+}$ mice. A) Pooled males and females linear measurements. B) Measurements in A expressed as a percentage using control as 100%. C) Males linear measurements. D) Measurements in C expressed as a percentage using control as 100%. E) Females linear measurements. F) Measurements in E expressed as a percentage using control as 100%. CTSK, $Ctsk^{Cre};DTA^{fl/+}$ nts

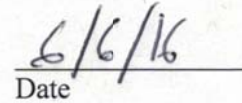
Publishing Agreement

It is the policy of the University to encourage the distribution of all theses, dissertations, and manuscripts. Copies of all UCSF theses, dissertations, and manuscripts will be routed to the library via the Graduate Division. The library will make all theses, dissertations, and manuscripts accessible to the public and will preserve these to the best of their abilities, in perpetuity.

Please sign the following statement:

I hereby grant permission to the Graduate Division of the University of California, San Francisco to release copies of my thesis, dissertation, or manuscript to the Campus Library to provide access and preservation, in whole or in part, in perpetuity.


Author Signature


Date